fortune Journals

Review Article

JOURNAL OF RADIOLOGY AND CLINICAL IMAGING

ISSN: 2644-2809

Real-time Tissue Properties from "Intelligent iSyringe" Pressure Transient Analysis

Jamie A. Chin

Abstract

A new imaging approach offering real-time quantitative local tissue information, complementing conventional X-ray, ultrasound, Catscan and MRI techniques that produce qualitative, global, subjective gray-scale descriptions is described. Its importance in medical clinical tissue characterization is underscored. Applications to manufactured (or cultivated) meat manufacturing, agricultural products, and pastry product formulation are also introduced. In short, pressure transients obtained and recorded during syringe injections and withdrawals can be interrogated using physics-based mathematical models using rapid real-time algorithms for permeability, anisotropy, compressibility, porosity and pore pressure. The general math boundary value problem, together with explicit solutions, is offered and applied to available datasets for swine and human subjects, plus newly acquired pressure transient data suites for uncooked meats, fruits, vegetables and pastry products. Also described in our exploratory investigations is a new software and hardware prototype system, consisting of a pressure transducer instrumented syringe, interpretation algorithms, auto-injector for flow rate control, wireless data acquisition and computer, together with suggested workflows for convenient, inexpensive, rapid porous media monitoring in routine tests, periodic monitoring and multiple syringe applications.

Introduction

Tissue Properties, Clinical Needs and Research Direction: The importance of conventional imaging methods, e.g., X-ray, ultrasound, Catscan and MRI, in modern medical diagnostics is paramount to an understanding of physical anomalies and root causes, tracking variations throughout the body, and monitoring changes in time. However, despite decades of use and numerous incremental improvements, significant limitations remain. For example, as shown in Figure 1, while they offer broad qualitative assessments on a global scale, all resulting gray-scale images must be subjectively interpreted by specialists and hence are subject to discretion and error.

Clinical importance of quantitative tissue characterization: For completeness, we summarize the roles of permeability, anisotropy, compressibility, pressure and porosity from several selected papers. Later, we will show how our iSyringe technology fulfills the needs described in this section.

Permeability: In the low Reynolds number "Darcy flow model" used, "permeability" describes the resistance a medium offers to flow. This resistance can be isotropic, that is, identical in all directions; or, it can be anisotropic, meaning that it is different in different directions; or, lastly, it

Affiliation:

The University of Hong Kong, Hong Kong

Corresponding author:
Jamie A. Chin, The University of Hong Kong, Hong Kong

Citation: Jamie A. Chin. Real-time Tissue Properties from "Intelligent iSyringe" Pressure Transient Analysis. Journal of Radiology and Clinical Imaging. 8 (2025): 72-87.

Received: May 28, 2025
Accepted: June 16, 2025
Published: June 17, 2025

Chin JA., J Radiol Clin Imaging 2025
DOI:10.26502/jrci.2809113

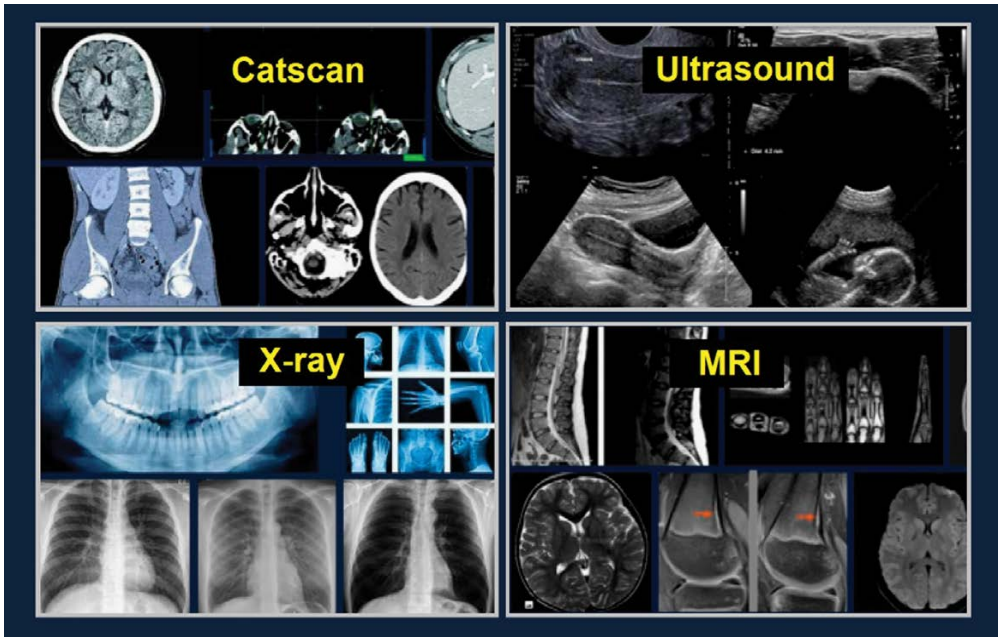

Figure 1: Conventional medical imaging methods.

can be transversely isotropic, with the permeability in two principal directions being identical and different from the third. In tissue media, permeabilities can be locally homogeneous (uniform) but generally heterogeneous (non-uniform) over larger space scales. Useful insights are offered in the Franke et al. (2009) paper "Permeability of technical and biological tissues." From its Abstract,

"The permeability of a material is described by the amount of substances (gases, liquids, particles) passing through pores and/or interstices of the material in a certain time. In medicine and biotechnology the permeability is given usually as the amount of water (ml x cm(-2) x min(-1)) permeating per area and time unit through the material. Vascular prostheses are described e.g. as high porous prostheses (e.g. Dacron: 1500-4000 (ml x cm(-2) x min(-1)) or as low porous prostheses (e.g. ePTFE: 200-1000 (ml x cm(-2) x min(-1)). The permeability of blood capillaries is characterized by the exchange of nutrients, metabolites and breathing gases. Capillary permeability and the transport of the permeates through tissues are the key processes for the supply of organs and tissues where especially the protein transport through tissues is described by diffusive and/or convective terms. The vascular permeability is governed by the permeability of the intimal endothelial cells. The major influence is exerted by the interendothelial binding which can change drastically in a very short time. This is demonstrated by the fast development of interstitial lung oedema in case of septical shock. The permeability is an integral indicator of tissue and organ function. It is possible to assess the permeability of native and engineered tissues precisely with a recently developed system. First results will be shown."

Tissue properties are more than definitions: Changes in properties imply good or undesirable changes in environment. For permeability, these provide diagnostic indicators for unseen events. In clinical work, permeabilities may increase or decrease; increases, for example, reflect local swelling. This subject has elicited strong interest over the years. The classic work of Duran-Reynals (1942), entitled "Tissue Permeability and the Spreading Factors in Infection," reviews tissue permeability measurement in different organs, for instance, pancreas, lungs, skin, muscle, and mammary and salivary glands. Experimental results for mice, rabbits and guinea pigs are given. Methods include color dye injection, India ink usage that monitors spreading, introduction of easily monitored toxic substances – the latter induces slight reactions, since local infections are an indicator of permeability. Essentially, permeability is in important factor in determining infection susceptibility. From the Abstract,

"Efforts by bacteriologists to clarify the importance of this field in infection, and the results of direct experiments by a few physiologists, have provided facts which form a basis for the concept of permeability of the connective tissue (C.T.). It would seem that all these facts could be properly ranged with or between those concerning cell permeability and capillary permeability. It will be shown that the permeability of the C.T. has a normal, constitutional state or tonus which can be increased by certain factors and decreased by others, and these fluctuations of permeability result in parallel fluctuations in the degree of the infection which may have a decisive bearing on the final issue of the process."

Yuan and Rigor (2010) in "Regulation of Endothelial Barrier Function, Chapter 3 – Methods for Measuring Permeability" reviews permeability measurement techniques.

Chin JA., J Radiol Clin Imaging 2025
DOI:10.26502/jrci.2809113

Aside from technical discussions, historical highlights on a rapidly evolving discipline are outlined. These include experiments on hind limbs of cats, amputated limbs of dogs and lungs of animals, direct flow and filtration experiments interpreted with Darcy's laws, applications of colored dyes to monitor spreading, optical Doppler velocimeters, microscopic fluorescent probes, electrical resistance, and so on. Such methods require extensive laboratory analysis. Despite the abundance of modern imaging tools, for example, sonic transducers measuring acoustic backscatter, and conventional X-ray, ultrasound, Catscan and MRI scanners, the methods are nonetheless expensive, inconvenient and qualitative. Gray-scale images require interpretation by experienced radiologists, who are generally in need of additional information on sex, weight, ethnicity, health and age to render usable conclusions.

Anisotropy: Anisotropy refers to property differences found in different directions, e.g., in wood samples, mechanical strength is stronger across the grain than along it. Similar considerations apply to muscle fibers. An interesting biological discussion is offered in Mitchell and Tojeira (2013)'s "Role of Anisotropy in Tissue Engineering." From its Abstract,

"Tissue engineering is a highly interdisciplinary field that requires the integrated expertise of clinicians, cell biologists, engineers and material scientists, to make progress in the development and deployment of biological substitutes that restore, maintain, or improve tissue function. The purpose is to provide the opportunities for tissue regeneration and organ replacement. Key advances in biological materials especially in the area of stem cells; growth and differentiation factors generate realistic opportunities to create tissues in the laboratory using an engineered extracellular matrix or scaffold and biologically active molecules. The scaffold acts as an artificial extracellular matrix and it needs to mimic the chemical composition and physical architecture of natural extracellular matrix to facilitate cell adhesion, proliferation, differentiation and new tissue formation. In this contribution we review the role of the scaffold system in promoting cell adhesion, proliferation and differentiation with respect to the anisotropic nature of the scaffold system. We address both the anisotropy which may exist at a microscopic or mesoscopic scale, for example the shape of pores as well as the molecular level interactions which may arise in a scaffold containing a molecular organization with a preferred orientation which may have been induced during the processing procedures used to prepare the scaffold. Of course some approaches to the preparation of scaffolds systems are inherently anisotropic, for example the wide-spread utilization of meshes prepared by electrospinning. In other words although the overall scaffold is isotropic, the basic elements in terms of an electrospun fibre is highly anisotropic in terms of its external form and possibly in terms of its internal structure. By reviewing the possible advantages of the inclusion of anisotropic elements in the scaffold we add to the knowledge base which allows scaffolds design to be optimised for specific tissue growth."

Another useful discussion on anisotropy is provided by Chanda and Callaway (2018)'s "Tissue Anisotropy Modeling Using Soft Composite Materials." From its Abstract,

"Soft tissues in general exhibit anisotropic mechanical behavior, which varies in three dimensions based on the location of the tissue in the body. In the past, there have been few attempts to numerically model tissue anisotropy using composite-based formulations (involving fibers embedded within a matrix material). However, so far, tissue anisotropy has not been modeled experimentally. In the current work, novel elastomer-based soft composite materials were developed in the form of experimental test coupons, to model the macroscopic anisotropy in tissue mechanical properties. A soft elastomer matrix was fabricated, and fibers made of a stiffer elastomer material were embedded within the matrix material to generate the test coupons. The coupons were tested on a mechanical testing machine, and the resulting stress-versus-stretch responses were studied. The fiber volume fraction (FVF), fiber spacing, and orientations were varied to estimate the changes in the mechanical responses. The mechanical behavior of the soft composites was characterized using hyperelastic material models such as Mooney-Rivlin's, Humphrey's, and Veronda Westmann's model and also compared with the anisotropic mechanical behavior of the human skin, pelvic tissues, and brain tissues. This work lays the foundation for the experimental modelling of tissue anisotropy, which combined with microscopic studies on tissues can lead to refinements in the simulation of localized fiber distribution and orientations, and enable the development of biofidelic anisotropic tissue phantom materials for various tissue engineering and testing applications."

Compressibility: In laymen's terms, compressibility is the capacity of a material sample to be altered in volume by increases or decreases in pressure. In thermodynamics and fluid mechanics, a more precise definition is used: compressibility is a measure of the relative volume change of a fluid or solid as a response to a pressure change. For example, applications, we might draw upon the Abstract in Nolan and Mcgarry (2015)'s "On the Compressibility of Arterial Tissue."

"Arterial tissue is commonly assumed to be incompressible. While this assumption is convenient for both experimentalists and theorists, the compressibility of arterial tissue has not been rigorously investigated. In the current study we present an experimental-computational methodology to determine the compressibility of aortic tissue and we demonstrate that specimens excised from an ovine descending aorta are significantly compressible. Specimens are stretched in the radial direction in order to fully characterise the mechanical behaviour of the tissue

Chin JA., J Radiol Clin Imaging 2025
DOI:10.26502/jrci.2809113

ground matrix. Additionally biaxial testing is performed to fully characterise the anisotropic contribution of reinforcing fibres. Due to the complexity of the experimental tests, which entail non-uniform finite deformation of a non-linear anisotropic material, it is necessary to implement an inverse finite element analysis scheme to characterise the mechanical behaviour of the arterial tissue. Results reveal that ovine aortic tissue is highly compressible; an effective Poisson's ratio of 0.44 is determined for the ground matrix component of the tissue. It is also demonstrated that correct characterisation of material compressibility has important implications for the calibration of anisotropic fibre properties using biaxial tests. Finally it is demonstrated that correct treatment of material compressibility has significant implications for the accurate prediction of the stress state in an artery under in vivo type loading."

Local pressures. Background pressures are relevant because they assist or impede fluid motions; large magnitudes can be detrimental. Aside from its obvious role in moving blood through arteries and veins, Carreau et al. (2011) in "Why is the partial oxygen pressure of human tissues a crucial parameter?" offers additional insights. From the Abstract, the authors note that,

"Oxygen supply and diffusion into tissues are necessary for survival. The oxygen partial pressure (pO2), which is a key component of the physiological state of an organ, results from the balance between oxygen delivery and its consumption. In mammals, oxygen is transported by red blood cells circulating in a well-organized vasculature. Oxygen delivery is dependent on the metabolic requirements and functional status of each organ. Consequently, in a physiological condition, organ and tissue are characterized by their own unique 'tissue normoxia' or 'physioxia' status. Tissue oxygenation is severely disturbed during pathological conditions such as cancer, diabetes, coronary heart disease, stroke, etc., which are associated with decrease in pO2, i.e. 'hypoxia'. In this review, we present an array of methods currently used for assessing tissue oxygenation. We show that hypoxia is marked during tumour development and has strong consequences for oxygenation and its influence upon chemotherapy efficiency. Then we compare this to physiological pO2 values of human organs. Finally we evaluate consequences of physioxia on cell activity and its molecular modulations. More importantly we emphasize the discrepancy between in vivo and in vitro tissue and cells oxygen status which can have detrimental effects on experimental outcome. It appears that the values corresponding to the physioxia are ranging between 11% and 1% O2 whereas current in vitro experimentations are usually performed in 19.95% O2, an artificial context as far as oxygen balance is concerned. It is important to realize that most of the experiments performed in so-called normoxia might be dangerously misleading."

The authors also note that,

"Oxygen is vital for living cells; it plays a fundamental role in their metabolism. However, the simple molecular diffusion of gases in tissues, as well as nutrients is not sufficient for the metabolic needs of large, complex and active multicellular organisms. Consequently, it is necessary to provide tissues and cells with optimal oxygen concentrations. […] Several strategies have been developed to maximize oxygen capture and oxygen transport into organs. In mammals, oxygen is absorbed by the lungs. Because of its poor solubility, oxygen is bound to haemoglobin which is packaged within red blood cells. A well-organized vasculature enables the delivery of oxygenated red blood cells to the tissues. The macrovasculature allows a rapid blood circulation and the microvasculature which irrigates each organ provides locally the optimal oxygen supply. A highly controlled oxygenation of cells is vital, particularly in animals with very high metabolic requirements. [Selected portions of text deleted] The present review is to exemplify how the oxygen partial pressure (pO2) in tissues influences the molecular and subsequent cellular behaviours."

Porosity: Porosity measures the "empty volume" in a spongy medium. Consider a simple sponge. If 30% of the volume is filled with holes, the sponge is 30% porous. High porosities in Darcy media need not imply ease of flow since pore spaces must be interconnected. Pore spaces that are poorly connected are low in permeability and do not support oil production in oil reservoirs. In biological applications, porous interconnected networks are important for cell nutrition, proliferation, and migration for tissue vascularization and formation of new tissues. Also, tissues with high porosity enable the effective release of proteins, genes, or cells and provide good substrates for nutrient exchange. An interesting paper dealing with porosity is offered by Loh and Choong (2013) in "Three-Dimensional Scaffolds for Tissue Engineering Applications: Role of Porosity and Pore Size." From the Abstract,

"Tissue engineering applications commonly encompass the use of three-dimensional (3D) scaffolds to provide a suitable microenvironment for the incorporation of cells or growth factors to regenerate damaged tissues or organs. These scaffolds serve to mimic the actual in vivo microenvironment where cells interact and behave according to the mechanical cues obtained from the surrounding 3D environment. Hence, the material properties of the scaffolds are vital in determining cellular response and fate. These 3D scaffolds are generally highly porous with interconnected pore networks to facilitate nutrient and oxygen diffusion and waste removal. This review focuses on the various fabrication techniques (e.g., conventional and rapid prototyping methods) that have been employed to fabricate 3D scaffolds of different pore sizes and porosity. The different pore size and porosity measurement methods will also be discussed. Scaffolds with graded porosity have also been studied for their ability to better

Chin JA., J Radiol Clin Imaging 2025
DOI:10.26502/jrci.2809113

represent the actual in vivo situation where cells are exposed to layers of different tissues with varying properties. In addition, the ability of pore size and porosity of scaffolds to direct cellular responses and alter the mechanical properties of scaffolds will be reviewed, followed by a look at nature's own scaffold, the extracellular matrix. Overall, the limitations of current scaffold fabrication approaches for tissue engineering applications and some novel and promising alternatives will be highlighted."

Conventional permeability imaging: In this paper, we focus primarily on "effective" or "spherical permeability," which we will define precisely later. We describe its measurement in detail, to include theoretical background, algorithms, software and syringe hardware prototype design, and importantly, the industry's first rapid, accurate, and convenient measurements for uncooked meats, fruits and pastries performed using our pressure transient approach. We will also discuss initial results for compressibility, porosity, local pressure and anisotropy. Again, our method provides quantitative localized information. Often, such information is sought by "zooming" into scans such as those offered in Figure 1 by altering contrast settings during data processing. While reasonable, enhanced areas will depend on the imaging method used and the wavelength distributions employed.

For permeability estimates, highly in demand as noted, quantitative approaches are available. Minimally invasive in vivo methods do not exist, although common but inconvenient ex vivo approaches using "hydraulic cells" are possible. These rely on the hydraulic formula $Q = (k/\mu)\, A\, \Delta P/\Delta L$ known from engineering physics describing actual flow and not pressure transmission from compressibility transients. A simple one-dimensional system is assumed, where a fluid of viscosity μ is literally forced through a sample of cross-sectional area A and thickness ΔL under a volume flow rate Q. The steady-state pressure drop ΔP is recorded and the permeability "k" is calculated. In practice, this requires a large sample, say circular slices 1-2 inches in diameter, 0.25 - 0.5 thick, which must be mechanically supported, plus accurate pressure and flow rate instruments operated over hour-long time scales as shown in Figure 2.

While "simple" and seemingly accurate, the above only apply to "isotropic" materials where permeability (resistance to fluid flow) k is identical in all directions. However, many porous media flow problems are "anisotropic," with different kx, ky and kz values in the x, y and z directions. Numerous animal and human tissues are actually "transversely isotropic," meaning that two principal horizontal directions with identical permeabilities "kh" are complemented by a third vertical permeability "kv." For the above flow cells, "h" and "v" flow directions must be aligned with the flow to obtain kh and kv individually. Thus, the above methods provide only approximate estimates and extensions method are not possible. This is not so with our Intelligent iSyringe.

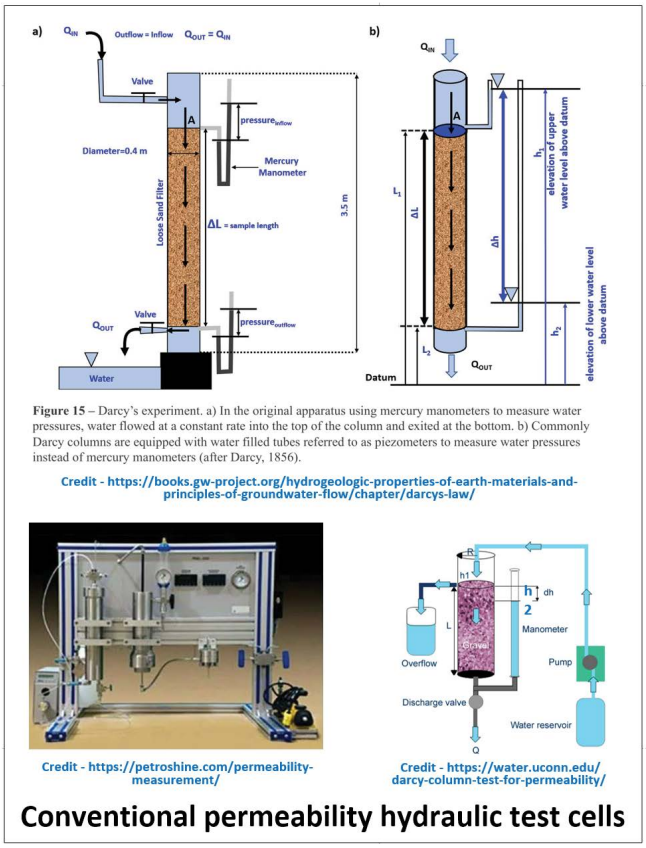

Figure 15 – Darcy's experiment. a) In the original apparatus using mercury manometers to measure water pressures, water flowed at a constant rate into the top of the column and exited at the bottom. b) Commonly Darcy columns are equipped with water filled tubes referred to as piezometers to measure water pressures instead of mercury manometers (after Darcy, 1856).

Credit - https://books.gw-project.org/hydrogeologic-properties-of-earth-materials-and-principles-of-groundwater-flow/chapter/darcys-law/

Figure 2: Conventional permeability test cells.

As we will show, a hierarchy of permeabilities is possible in principle, requiring upgraded instrumentation whose design principles are now known.

Other mechanical instruments (not described here) are needed to measure anisotropy (directional dependence), compressibility (change in volume under pressure loads), porosity (percentage volume) and background pressure. With iSyringe, predictions for these properties automatically follow from the same pressure permeability analysis. Thus, estimates for all the cited properties are available from a rapid, inexpensive, convenient quantitative method, similar in concept to standard and convenient blood tests or blood pressure measurements. These provide a suite of information that is invaluable in concert with physicians' independent assessments. These properties help answer key diagnostic questions. How deep is the swelling? How rapidly is a tumor growing or receding? Where should medicines be injected for optimal drug delivery? And what corrective plans are suggested?"

Intelligent iSyringe Introduction and Interpretation Algorithms

Syringe injections and withdrawals are as old as modern medicine. Laymen often view syringes as commodity tools, but this perspective is not quite correct. Numerous designs

Chin JA., J Radiol Clin Imaging 2025
DOI:10.26502/jrci.2809113

exist, depending injectate viscosity, net dosage and fluid flow rate properties. These designs can be adapted for various iSyringe purposes. Pharmaceutical companies are interested in pressure reactions and, in particular, pain thresholds responsible for patient discomfort. Example recent studies include Doughty et al. (2016) and Woodley et al. (2022), where "syringe pressure versus time" curves are presented. However, these studies focused more on maximum steady pressures rather than transient values found in "pressure buildup" (increasing with time) and "drawdown" (decreasing) limits. Transients hold the key to tissue properties prediction because time variations are affected and controlled by these properties. We will extract these properties from detailed measured pressure transients. Ideally, this is addressed using inexpensive, convenient, real-time instruments that can be used repeatedly in monitoring, while furnishing useful, immediate, real-time diagnostic information to physicians and researchers.

Chronological development: Fortunately, for low Reynolds number porous media flows, the centuries old "Darcy flow model" is available, successfully used in civil engineering (dam construction and soil mechanics), petroleum exploration (underground "formation testing"), and chemical engineering (filtration studies). Of particular interest is "formation testing," an underground oil exploration application where a "giant syringe" placed in miles-deep wells measures earth properties related to ease of flow and economic viability. Weighing thousands of pounds with twenty feet lengths, it withdraws and injects test fluids into porous rock under high pressures (10,000-20,000 psi) to produce flow rates up to 100 cc/sec. Recorded pressure transients are used to predict permeability and compressibility. While large differences in scale and visual appearance are found between "formation testers" and our "Intelligent iSyringe," as shown in Figure 3, any underlying physics-based differences are nominal. Darcy's formulation is mathematically summarized in Figure 4 for both problems, where the "forward analysis" equations appear at the top, while the "inverse problem" is conceptually summarized at the bottom. The "giant syringe" can be scaled down to sizes suitable for office use. Key ideas are developed in Chin and Chin (2023) and Chin, Chin and Zhuang (2024), and here, our prototype software and hardware system, together with test results for different sample types, are presented.

Mathematical approach: In our analysis, we consider general "transversely isotropic" (anisotropic) media, often found in human and animal tissue, as well as in underground petroleum exploration applications, where "horizontal kh" and "vertical kv" denote characteristic permeabilities or resistances to fluid flow. A layered medium is described by three "principal axes," with two pointing within the layer in horizontal x and y directions and the third oriented perpendicularly to the layer in the z direction. An "effective" or "spherical permeability," arising from the formulation in Figure 4, is often used and defined by $keff = kh^{2/3}kv^{1/3}$. These descriptions also apply to "isotropic" media, in which case kh and kv are identical. Two other definitions are also used. A syringe needle oriented normal to the layer possesses "zero dip angle, δ" while δ = 90 deg describes a needle axis almost parallel to the horizontal plane. "Mobility ratios" are introduced by kh/μ, kv/μ and keff/μ where μ is the injectate viscosity obtained from independent rheometer measurements.

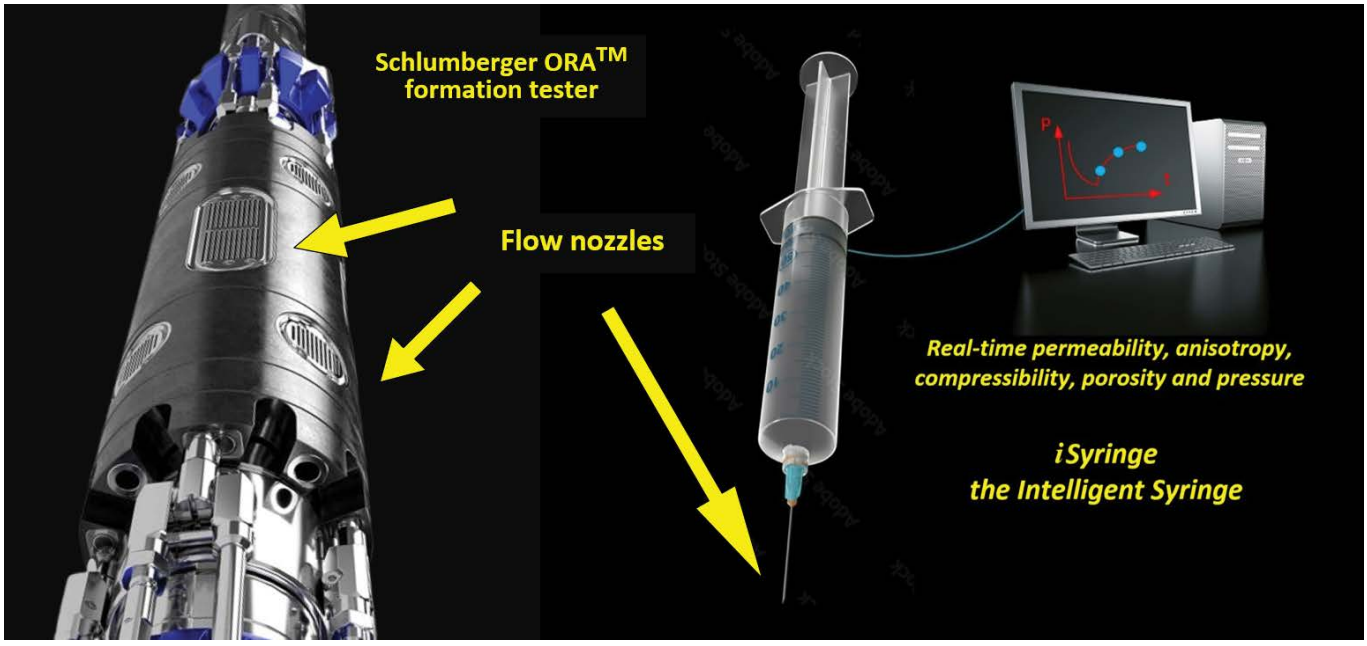

Figure 3: Oil industry "formation tester" (with retracted nozzles shown) and "Intelligent iSyringe" system.

Chin JA., J Radiol Clin Imaging 2025
DOI:10.26502/jrci.2809113

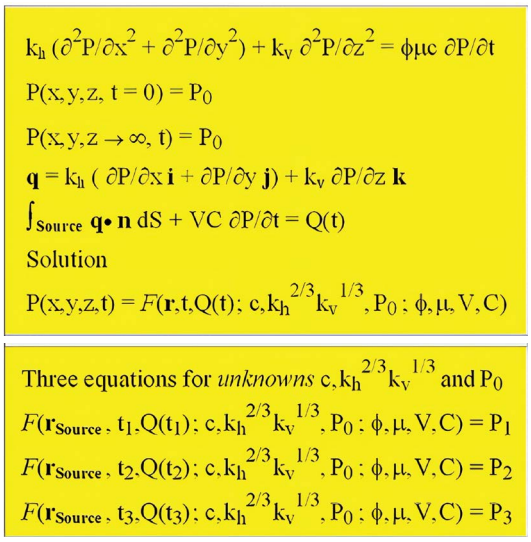

Figure 4: Darcy formulation, "forward" (top) and "inverse" (bottom) models. Note compressibility "c" refers to expansion in tissue media while "C" represents cushioning effect in syringe and accompanying flowline. The iSyringe measures effective tissue permeability Keff, but "c" only when it is not dominated by high compressibility air in its flowlines. Thus, in our experiments here, calculations refer to syringe air. Tissue compressibilities require blood withdrawals where air is not present in experimental setup.

The "forward problem" in Figure 4 predicts the time-dependent pressure response P(x,y,z,t) when kh, kv and additional constant parameters are prescribed. These include φ (porosity), μ (fluid viscosity), c (medium compressibility), C (syringe vessel compressibility), V (syringe vessel and flowline volume), and P_0 (initial or farfield local pressure). The first three lines at the top of Figure 4 summarize the partial differential equation, and the supplementary farfield and initial auxiliary conditions used. The fourth and fifth line describe the mechanics of fluid injection and withdrawal, where Q(t) is the volume flow rate. The net pressure P(x,y,z,t) combines medium and syringe vessel fluid responses. It can be shown that the product "VC" controls the width of the time window over which the transient process occurs. If a process reaches steady-state too rapidly, to the extent that accurate measurements cannot be obtained, V can be increased by increasing flowline length (that is, insertion of a long tube between syringe and auto-injector, or the introduction of highly compressible air into the syringe body).

It is also important that, whatever the value of VC, predictions for permeability will remain unaffected. The "inverse problem," by contrast, solves for fluid and medium properties when three discrete (pressure, time) data points along a transient curve are available. Inverse procedures, in this paper, form the basis for "Intelligent iSyringe" approaches to high resolution local imaging, and so, must be carefully designed and rigorously validated. Math solutions are available in the prior cited work. Our validation was performed as follows. The forward model, based on an exact analytical solution to the formulation in Figure 4, was used to create "patient data" where assumed input properties were entered into the transient pressure creation software. Then, three discrete sets of "pressure, time" points selected arbitrarily from a calculated transient curve were inputted into an independently derived inverse solver, with the objective being accurate prediction of those properties used in the forward solver. We now describe pressure transient solutions and validations in present applications contexts.

Pressure transient analysis basics. The complete exact, analytical solution to the forward problem in Figure 4 is presented in the book *Biofluids Modeling – Methods, Perspectives and Solutions* (Chin and Chin, 2023). There, P(x,y,z,t) is expressed in terms of "complex complementary error functions," and early-time as well as late-time asymptotic solutions are developed from the solution. These exact solutions, the inverse properties prediction problem, and the validation procedure outlined were originally developed in support of underground oil and gas exploration. These formed the basis for successful decades-long commercial services for several international oil companies. The success of the forward and inverse solutions and validation procedures provided the impetus behind the Intelligent iSyringe, as both rock formations and tissue applications represent instances of porous media flow. While these are hardly similar, at least visually, they do represent comparable porous media events when viewed dimensionlessly. That is, flow phenomena behind formation testers pumping fluids at dozens of cc/sec, under high 20,000 psi pressures into "hard rock" do not differ significantly from syringe pumps pumping at tenths of a cc/sec, under 10-100 psi pressures into "soft tissue."

In "scaling down" formation tester physics to table-top syringe scale, careful redesign is required. For example, in petroleum applications, "flowline volume" (or, V in the product "VC") internal to the tool must be reduced to minimize the hours-long time scale of the transient process. This is essential because hours to day-long wait times result in extremely expensive, million dollar drilling operations. On the other hand, syringe measurements often occur so rapidly that relevant activities are completed within seconds, rendering accurate data acquisition impossible. Consequently, iSyringe design must "increase the C in CV" (by using air within the syringe body), "increase V in VC" (by lengthening the flexible tubing joining syringe and auto-injector), or both. Fortunately, permeability predictions are unaffected by the value of the VC product. These considerations are described in Chin and Chin (2023), where sketches used in patent applications show different possible designs.

Until early in 2023, our understanding of tissue dynamics relied only on dimensionless estimates and expectations that porous flow phenomena in rocks and tissues follow similar qualitative trends. Only experiment could confirm or refute our ideas. We now explain why and how our methodologies

Chin JA., J Radiol Clin Imaging 2025
DOI:10.26502/jrci.2809113

evolved. When a formation tester or syringe injects fluid into sample media at a prescribed flow rate, pressures increase with time until steady-state levels are achieved. This creates a so-called "pressure buildup." If, however, injection terminates at some point in time, pressures will not only stop increasing – they will, as a consequence, reduce in level resulting in a "pressure drawdown." On the other hand, if the formation tester or syringe withdraws fluid, or withdraws fluid and then stops, the pressure sequence just described is reversed. Now, the scenarios just described appear in Figure 5 and are consequences of math solutions to the forward problem. These curves are well known and substantiated from decades of oil industry experience. But while comforting, similar evidence for live animal and human subjects was not available until we identified two pharmaceutical industry papers. The authors, interested only in steady "pressure plateaus" associated with pain thresholds, published experimental curves for live swine and human in their entirety that are consistent with Figure 5.

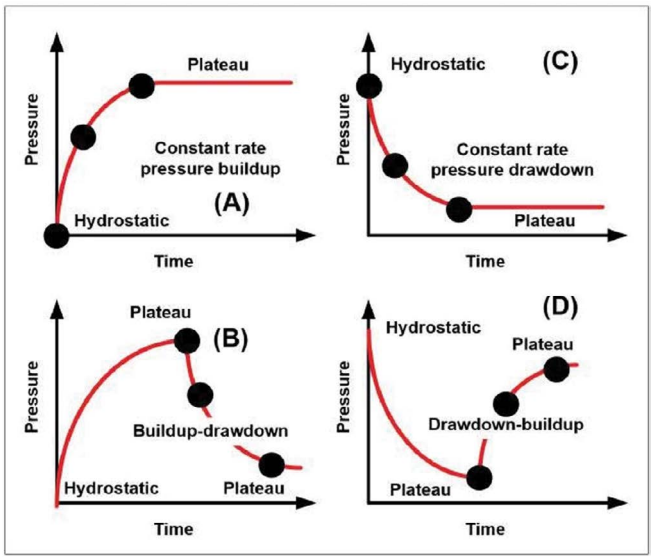

Figure 5: Transient pressures in porous media pumping applications.

Promising initial calculations: Again, the unsteady portions of the entire pressure transient curve are strongly dependent on tissue parameters, and our inverse equations attempt to recover parameter values when limited (pressure, time) datasets are available. The inverse summary in Figure 4 essentially inverts the available forward analytical to provide explicit tissue results. The red experimental swine results in Figure 6 due to Doughty et al. (2016) definitively show behavior consistent with Figure 5, with the exception of outlier Curves A and C. The needle radius (needed for syringe tip boundary conditions in Lines 4 and 5 of Figure 4 was not available. We therefore considered a range of radii, and concluded from inverse estimates that permeabilities fell in the range 100-300 md. This is not unreasonable considering beach sand is 1,000 md while hard rock is 0.1 md (few reliable permeability estimates are available in the decades-old medical literature). The recent work of Woodley et al. (2022) shown in Figure 7 provides human thigh data averaged over two dozen subjects. Again, needle sizes were not recorded, and our permeability estimates assuming one particular gauge size predicted permeabilities near 40 md. As in the Doughty experiment, this is not unreasonable and falls within credible ranges. Note that our inverse method actually predicts the "effective mobility" keff/μ where μ is viscosity. Multiplication by an assumed value of 1 cp (the viscosity of water) led to our 40 md. Detailed calculations for both experimental datasets are analyzed in Chin and Chin (2023) and Chin, Chin and Zhuang (2024). That permeability values and curve shapes were consistent with theory and oil exploration results supports our use of Darcy flow analysis.

Software and hardware integration, and system prototype development: The forward and inverse mathematical formulations in Figure 4 were packaged into Windows applications as shown in Figures 8 and 9. The prototype system appears in Figure 10.

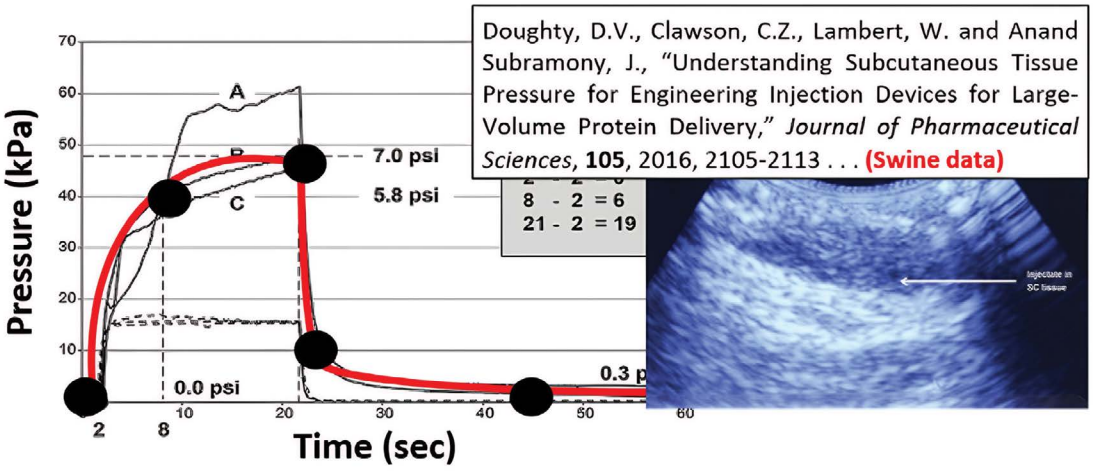

Figure 6: Pressure transient dataset from swine experimental evaluation (red curve selected for data analysis, black outliers with slope discontinuities discarded).

Chin JA., J Radiol Clin Imaging 2025
DOI:10.26502/jrci.2809113

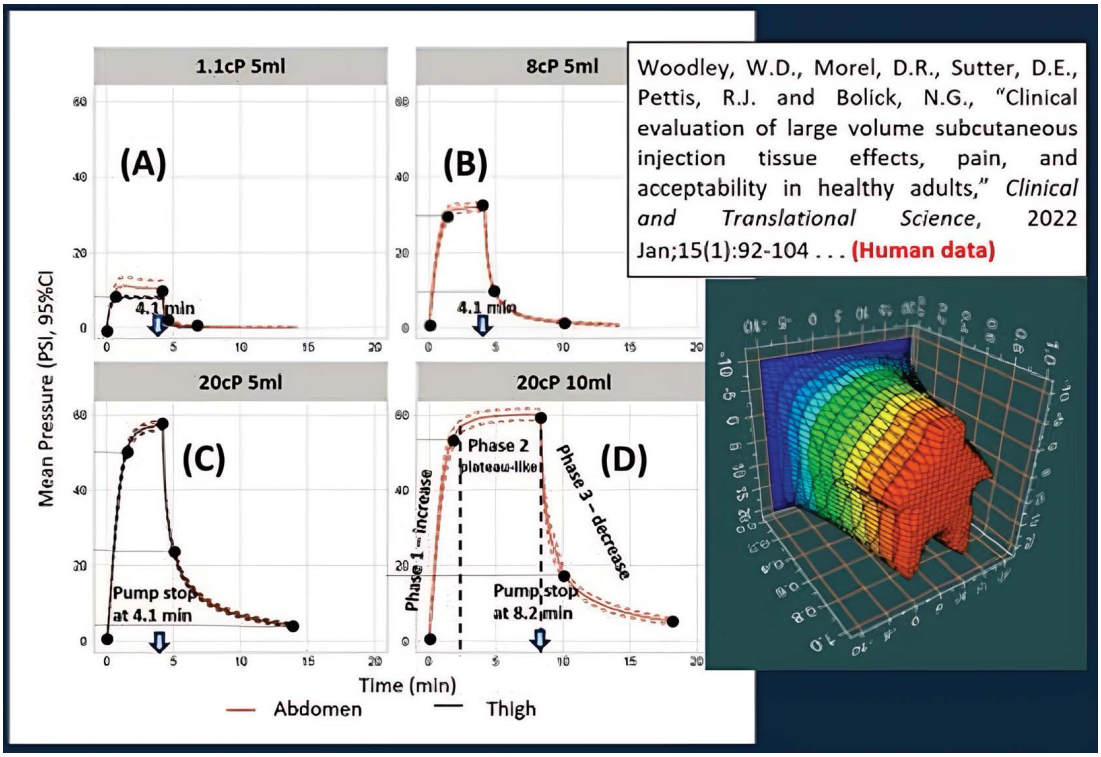

Figure 7: Pressure transient live human dataset (inset suggests "full body, tissue, vein and arterial simulations" anticipated in future Computational Fluid Dynamics (CFD) modeling work.

Detailed Pressure Test Suites and Predictions

The importance of permeability is accepted in civil engineering and soil mechanics, and test cells like those in Figure 2 are used in laboratory analyses. In petroleum exploration, rapid "formation testing" using pressure transient analysis have proven useful for two decades, however, the method has not been demonstrated outside of geoscience applications. This paper describes first exploratory results

Example raw beef initial test: The workflow used to evaluate a sample appears in Figure 11. The total desk time required to test, evaluate and document each run is five minutes. Outputs, available within seconds, are shown in Figures 12 and 13 for a raw beef sample. To process the outputs in the black computer screens, the formulas "Effective permeability (md) = Effective spherical mobility (md/cp) x air viscosity (cp)" and "Compressibility (1/psi) = 'Displayed number' x cc/FlolineVol" are used. Here room air was used as the working fluid, for which a viscosity of 0.018 cp and a compressibility of 0.068/psi are known at room temperature and pressure. Further analysis follows Figure 13.

Note from Figure 12 that the red data points used for inverse analysis were selected arbitrarily. Also, buildup processes are affected by initial needle movements, while later drawdown is often subject to debris trapped within the needle. Thus, properties predictions are not expected to perfectly agree. From the above data, spherical mobilities are close at 4,787 md/cp and 5,476 md/cp, or 5,132 md/cp on average. Multiplication by a viscosity of 0.018 cp gives keff = 92.4 md, a reasonable small value. For reference, beach sand permeability is approximately 1,000 md, while that of low permeability rock ranges from 0.1 – 10 md. The "Display numbers" for "Compressibility (1/psi)" are 3.765 and 3.535, or 3.650 averaged. The measured "flowline volume V" within the large syringe body attached to the autoinjector and long flexible tubing is about 50 cc. Dividing 3.650 by 50 gives an air compressibility of 0.073/psi, which compares favorably with 0.068/psi for the known air compressibility at room temperature and pressure. For our injection work, this "0.068" represents air within the syringe, since high air compressibilities dominate those in the tissue. To measure tissue compressibility, blood must be withdrawn from tissue and air related distractions must not be present.

Additional permeability test suites: It is known that "beef" is far from unique, with eight main "cuts," namely chuck, rib, loin, round, flank, plate, brisket and shank also available. Within any one, tissues are nonuniform, contain fatty streaks, with variabilities in texture. Additional beef tests demonstrated anticipated variations in permeability results. Thus, pressure analysis can be used to assess meat products rapidly and differences between meats from older and younger cattle can be conveniently obtained. While we initially focused on medical imaging and clinical objectives, and still do, interest in our methods found support from "manufactured or cultivated meat" producers, driven by economic and climate incentives to reduce dependence on

Chin JA., J Radiol Clin Imaging 2025
DOI:10.26502/jrci.2809113

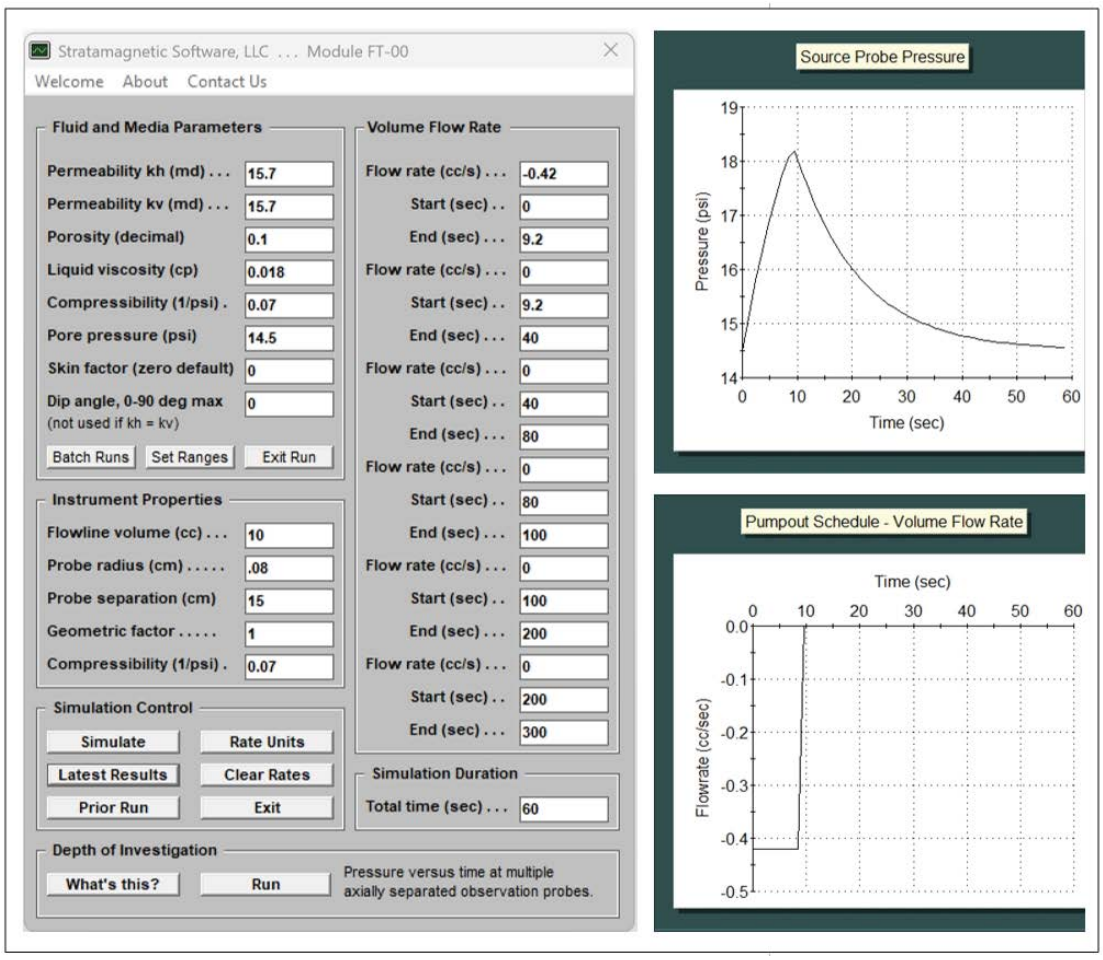

Figure 8: Forward pressure transient "patient data" creation module. Needle pressures (upper curve) and volume flow rates (lower curve) shown.

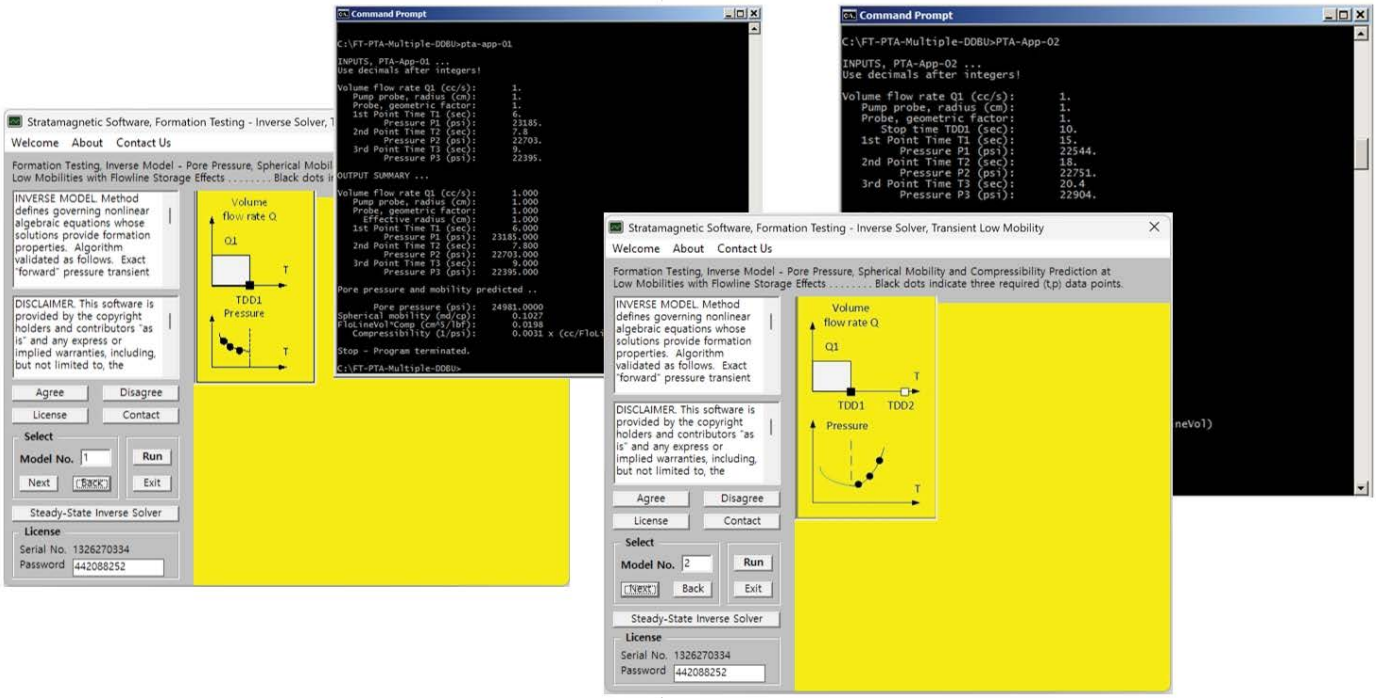

Figure 9: Inverse pressure transient modules, initial time curve (left) and final time curve (right) interpretation applications.

Chin JA., J Radiol Clin Imaging 2025
DOI:10.26502/jrci.2809113

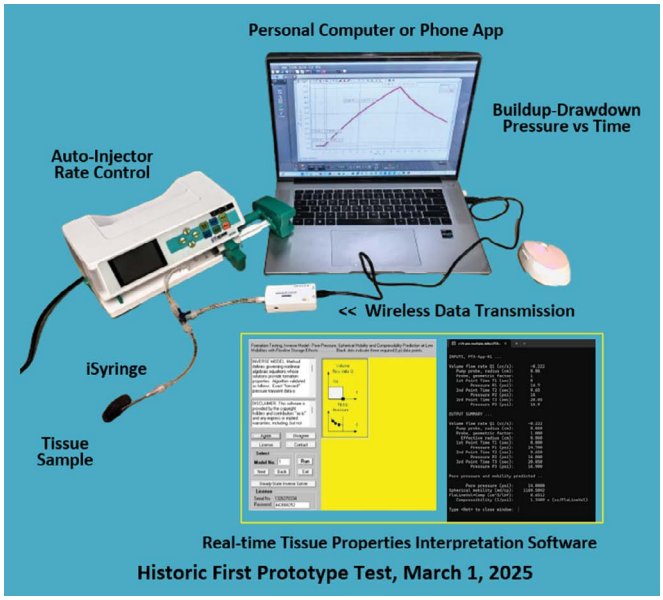

Figure 10: Prototype system, autoinjector, pressure transducer instrumented syringe, wireless data acquisition units and tissue sample (left), computer with forward and inverse software (top right), and software with menu and solutions screens (bottom right).

animals, agricultural fruit and vegetable producers who see permeability for its use in ripeness and harvesting applications, and interestingly, from pastry manufacturers, who currently use permeability to assess interior texture (important to the eating experience) and exterior crustiness (vital to product shelf life). Thus, our exploratory studies focused on broad ranges of products, with results catalogued in Figures 14-A to 14-E. For such testing, we used air as the injection fluid, due to its low cost and availability, at 0.5 cc/sec and below. We emphasize that for in vivo animal and human tissue tests, the use of air is not acceptable out of safety concerns. For such applications, pure saline solutions can be used for injection, while blood withdrawal from tissues themselves would naturally see blood as the working fluid without air cushioning effects.

Data analysis and comments. Each of the samples evaluated, from the spatially non-uniform, fibrous and likely anisotropic sample collection, was tested at multiple points. Because these were not uniform following the math model in Figure 4, permeability predictions were not often identical, but did consistently fall into an anticipated small 0.1 – 500 md range with small md values. Measured pressure transient traces all take the shapes in Figure 5, obtained from theory and from familiar petroleum exploration field measurement results. All of the results of Figure 14-E are satisfactory from this perspective. Many pressure buildups and drawdowns are noticeably straight lines. This is a hallmark of "low permeability," as is known from porous media theory in *Formation Testing – Pressure Transient and Contamination Analysis* from Chin et al. (2014) and papers referenced therein.

The permeability range quoted was obtained from buildup curves, but drawdown calculations were not as successful. As noted, these did not fall significantly and return to pre-pumping levels as modeling predicts, as would be expected physically when injections are terminated. This incomplete drawdown may arise from debris jammed in needle passages or altered media from fluid injection. The effect is also found in petroleum engineering operations. There, it is common for rock debris to accumulate within nozzle passages, thus blocking flow – in formation testing instruments, all having sizable flowline diameters, mechanical scrapers are actually installed to loosen and remove cuttings from the flowline. However, this is not possible with small sized syringe needles. So at present we recommend only buildup testing.

Another concern arises conceptually from needle diameter considerations. An interesting question raised by math theorists concerns the distance between two points, say a single step along a country road. A simple ruler measurement might indicate "one meter," however, to a microscopic insect navigating the millions of "ups and downs" along crests and troughs lodged between numerous grains in typical samples

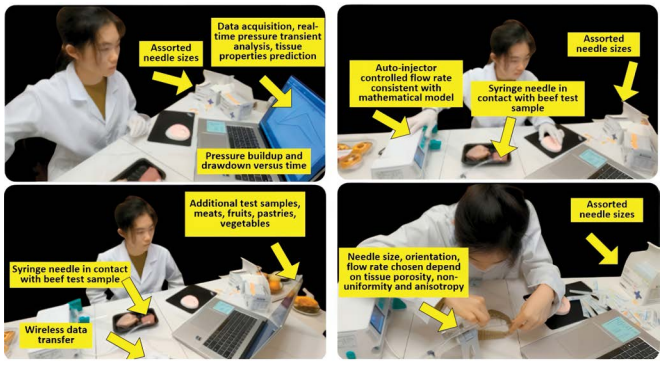

Figure 11: Tissue analysis workflow, total desk time required, less than five minutes per sample.

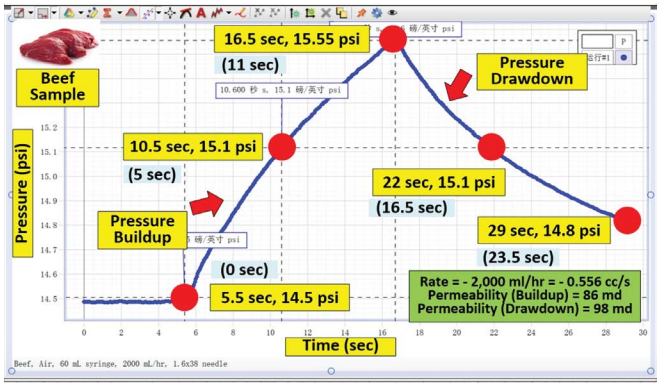

Figure 12: Typical buildup and drawdown pressure transient curves for uncooked beef sample (top left, white screen), buildup interpretation (center black screen) and drawdown analysis (right black screen). Latter screens are magnified in Figure 13 for clarity. Inverse math model software described in Chin, Chin and Zhuang (2024).

Chin JA., J Radiol Clin Imaging 2025
DOI:10.26502/jrci.2809113

```
Volume flow rate Q1 (cc/s):       -0.556
   Pump probe, radius (cm):        0.08
   Probe, geometric factor:        1
   1st Point Time T1 (sec):        0
         Pressure P1 (psi):        14.5
   2nd Point Time T2 (sec):        5
         Pressure P2 (psi):        15.1
   3rd Point Time T3 (sec):        11
         Pressure P3 (psi):        15.55

OUTPUT SUMMARY ...

Volume flow rate Q1 (cc/s):       -0.556
   Pump probe, radius (cm):        0.080
   Probe, geometric factor:        1.000
     Effective radius (cm):        0.080
   1st Point Time T1 (sec):        0.000
         Pressure P1 (psi):       14.500
   2nd Point Time T2 (sec):        5.000
         Pressure P2 (psi):       15.100
   3rd Point Time T3 (sec):       11.000
         Pressure P3 (psi):       15.550

Pore pressure and mobility predicted ..

       Pore pressure (psi):  0.1400E+02
Spherical mobility (md/cp):  0.4787E+04
FloLineVol*Comp (cm^5/lbf):  0.2429E+02
   Compressibility (1/psi):  0.3765E+01 x (cc/FloLineVol)
```

```
   1st Point Time T1 (sec):        11
         Pressure P1 (psi):        15.55
   2nd Point Time T2 (sec):        16.5
         Pressure P2 (psi):        15.1
   3rd Point Time T3 (sec):        23.5
         Pressure P3 (psi):        14.8

OUTPUT SUMMARY ...

Volume flow rate Q1 (cc/s):       -0.556
   Pump probe, radius (cm):        0.080
   Probe, geometric factor:        1.000
     Effective radius (cm):        0.080
    Stop time TDD1 (sec):       11.000
   1st Point Time T1 (sec):       11.000
         Pressure P1 (psi):       15.550
   2nd Point Time T2 (sec):       16.500
         Pressure P2 (psi):       15.100
   3rd Point Time T3 (sec):       23.500
         Pressure P3 (psi):       14.800

Pore pressure and mobility predicted ..

       Pore pressure (psi):  0.1400E+02
Spherical mobility (md/cp):  0.5476E+04
FloLineVol*Comp (cm^5/lbf):   0.2281E+02
   Compressibility (1/psi):   0.3535E+01 x (cc/FloLineVol)
```

Figure 13: Pressure buildup interpretation (left) and drawdown analysis (right) solution screens.

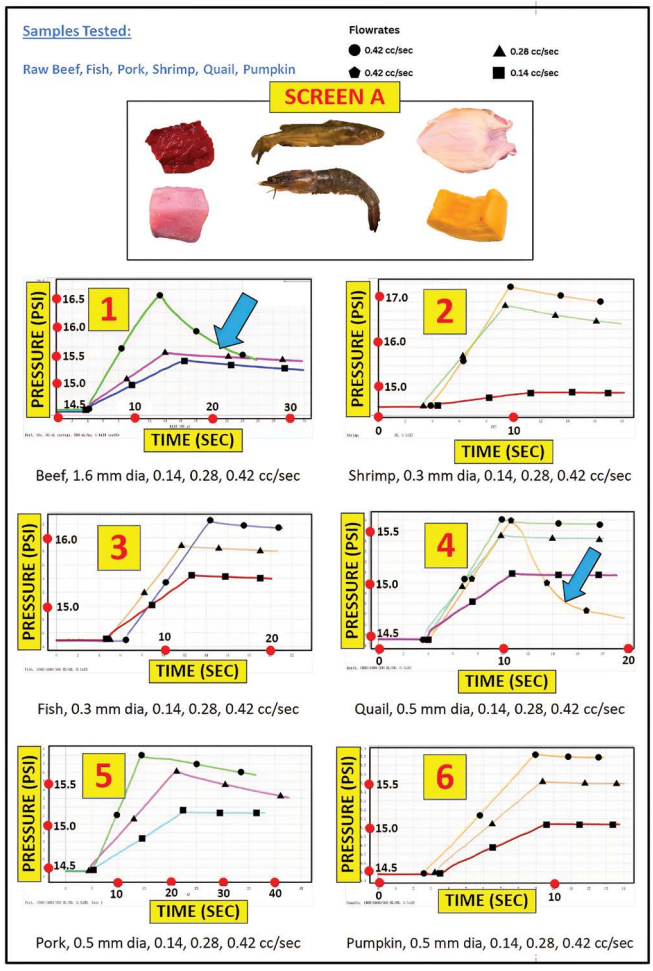

Figure 14A: Raw beef, fish, pork, shrimp, quail and pumpkin pressure data. Blue arrows are used to indicate good pressure drawdowns versus debris clogging and tissue damage effects.

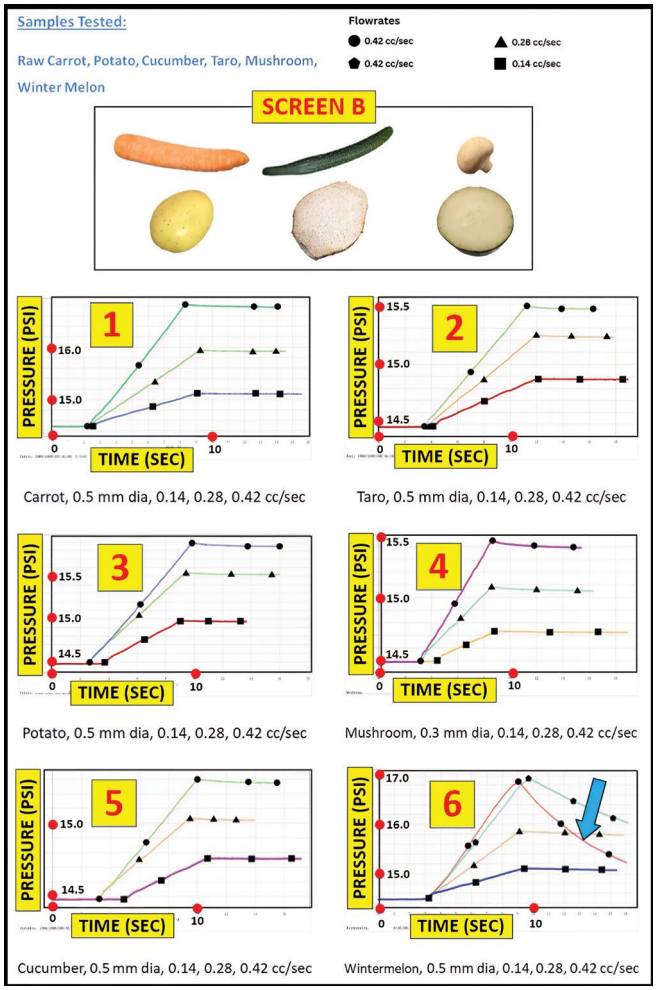

Figure 14B: Raw carrot, potato, cucumber, taro, mushroom and winter melon pressure data.

Chin JA., J Radiol Clin Imaging 2025
DOI:10.26502/jrci.2809113

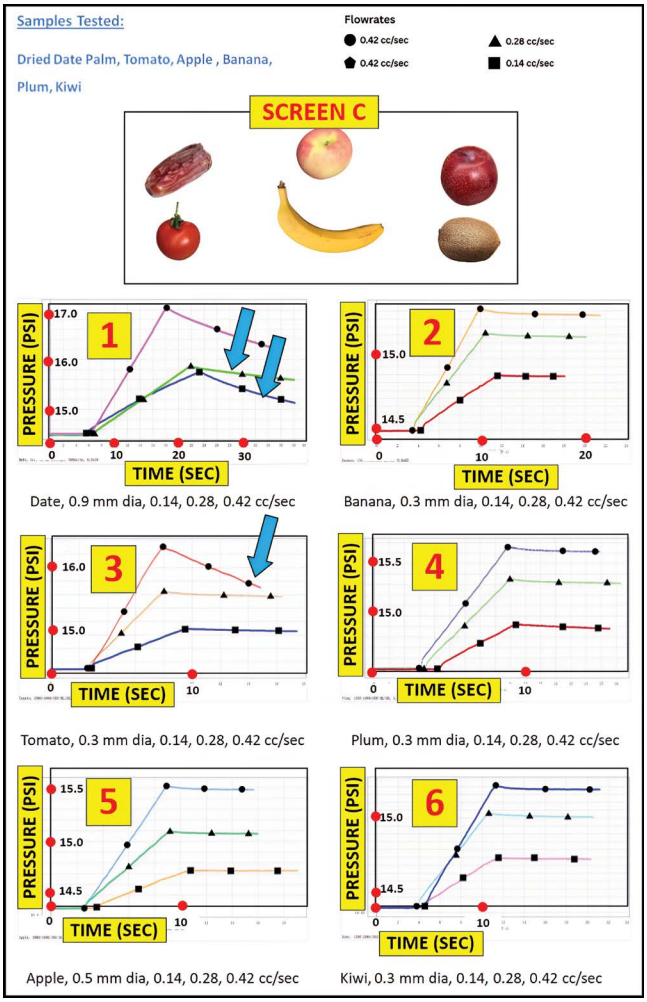

Figure 14C: Dried date palm, tomato, apple, banana, plum and Kiwi pressure data.

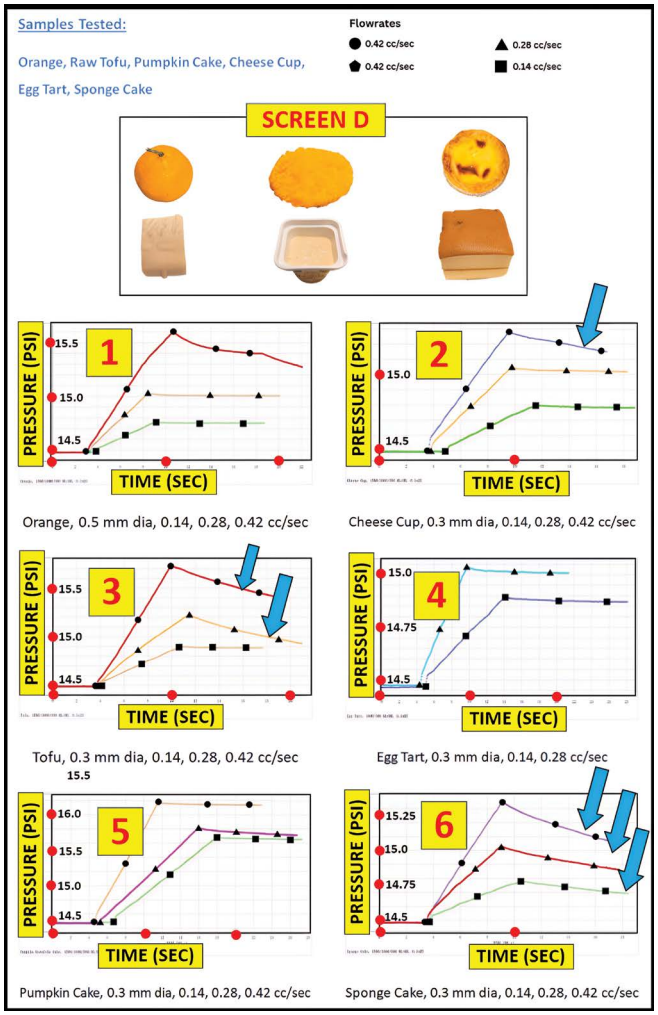

Figure 14D: Orange, raw tofu, pumpkin cake, cheese cup, egg tart and sponge cake pressure data.

would answer otherwise. Thus, answers also depend on the mode of measurement. Typical petroleum applications are highlighted below in Figure 15, where nozzle designs are selected accordingly as formations are comprised of loose sand, solid porous rock, or naturally fractured media. In syringe applications, heterogeneities include naturally occurring non-uniformities, small fatty streaks and fibrous muscle anisotropies – additional degrees of freedom are introduced by needle designs (blunt versus beveled puncture points) and entry angle. The end physical result of these effects must be accounted for in data interpretation, with laboratory calibration results described by "geometric factors" published together with tools sold by manufacturers. This will be required of syringe devices.

While not apparent to laymen, commercial syringe designs vary broadly, and dozens if not hundreds are offered by manufacturers for different scenarios depending on anticipated flow rate, injectate viscosity, total dosage, and of course, patient pain thresholds. Clinicians are aware of these considerations, as are petroleum engineers in oil well drilling in formation testing planning. In Figure 14, which highlights only a small group from our test program, we experimented with different needle diameters (with correspondingly different flow rates) for each sample studied. Tests were performed at multiple nearby locations where possible, but these often led to different permeabilities due to reasons cited previously. The top beef curve in Figure 14-A1 and one quail curve from Figure 14-A4 illustrate curvatures similar to those of Figure 5 due to relatively high permeabilities, compared with, say the straight line banana curves of Figure 14-C2 obtained for very low permeability samples. Again, straight drawdowns with insufficient pressure drop likely result from clogged needle passages. In petroleum applications, high injection rates may similarly damage or fracture formations, leading to ambiguous results. However, when pressures are recoverable during oilwell drilling, they do provide excellent estimates for farfield reservoir pore pressure – high pressures are essential to economic viability, allowing oils and gases to naturally rise to the surface through wells without artificial lift. For our experiments, good pressure recoveries are indicated by thick blue arrows, but any "pore pressure" extrapolation would have simply yielded starting

Chin JA., J Radiol Clin Imaging 2025
DOI:10.26502/jrci.2809113

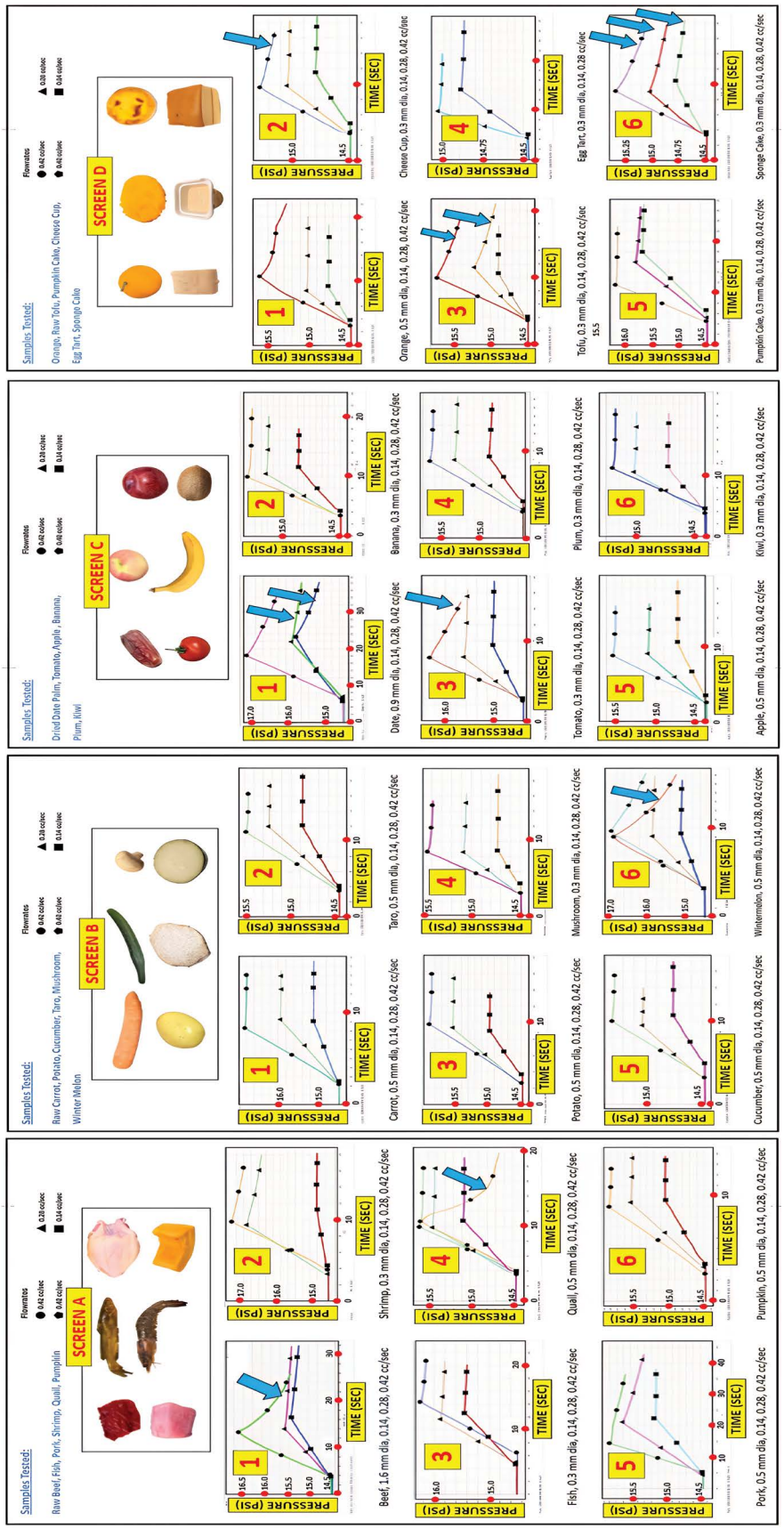

Figure 14E: Cumulative pressure data from Screens A, B, C and D. In general, pastries possessed the highest permeabilities, followed by fruits, then meats and finally raw vegetables.

Chin JA., J Radiol Clin Imaging 2025
DOI:10.26502/jrci.2809113

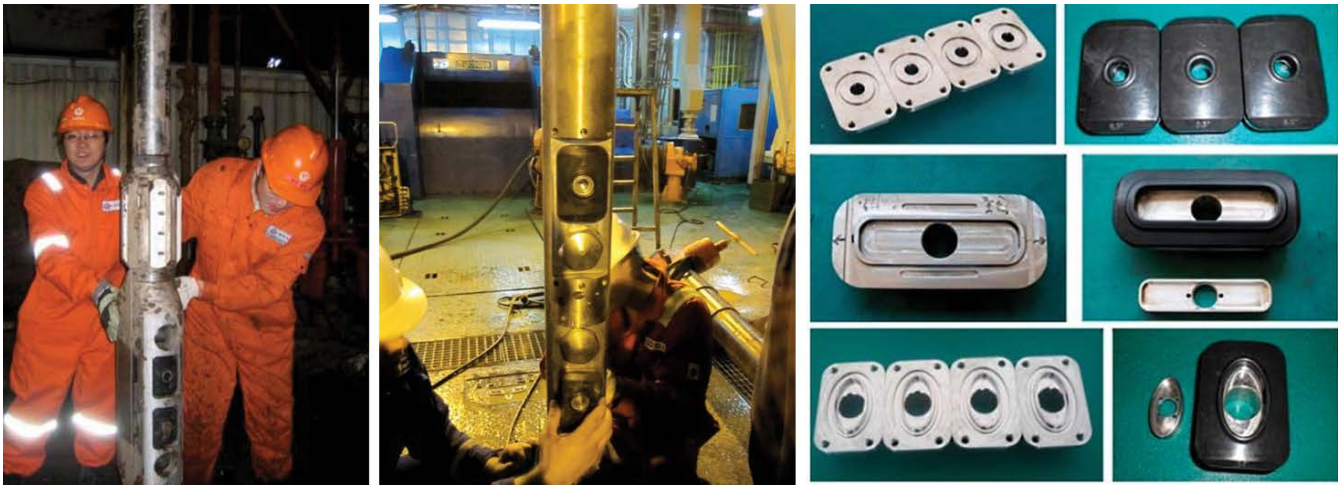

Figure 15: Typical formation tester lowered into well (left and center), with different nozzle designs (right) for contrasting rock formations) analogous to different needle diameters used in Figure 14.

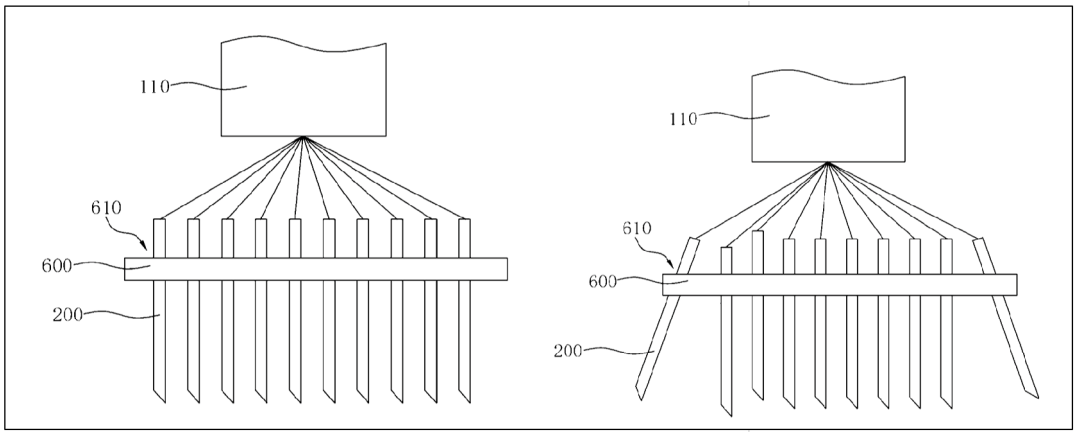

Figure 16: Possible multi-needle array syringes, enabling multiple depths and angles.

pressures in our test facility (our isolated "open air" samples were tested in a 40th Floor laboratory where measured ambient pressures of 14.5 psi are seen the plotted graphs). If animal tests had been conducted in vivo, slightly higher local pressures will be found which vary with location. These are useful in identifying and monitoring health anomalies, e.g., tumor growth and swelling – pressures so obtained differ from blood pressure readings obtained in physicians' offices, which measure only macroscopic averages during periods of rest and activity.

Finally, we would like to emphasize that, since permeability is a tissue property, its value should not depend on needle size or flow rate. However, differences are observed experimentally. These arise because, for example, higher flow rates may alter the tissue medium, by damaging it or compacting it in an unpredictable manner. Of course, deviations from ideal math predictions also assist in diagnosis.

We have discussed permeability, compressibility and pore pressure so far, and now turn to porosity and anisotropy. Mathematical discussions and summaries are offered in Chin, et al. (2014) and Chin, Chin and Zhuang (2024) and readers are referred to those publications for details. The boundary value problem formulation in Figure 4 applies to transversely isotropic porous media, where two horizontal principal axis directions x and y are associated with a kh permeability, while a third vertical axis in the z direction is associated with kv. When single needle iSyringes are used, either for injection or blood withdrawal, the quantity predicted from Figure 4 inverse formulations is actually the "effective or spherical spherical mobility," that is, keff/μ where μ is the separately measured Newtonian viscosity, with a similar effective permeability satisfying $keff = kh^{2/3}kv^{1/3}$. To obtain the porosity φ, the viscosity μ is first measured from conventional rheological instruments; then keff is calculated from the inverse software data in Figure 13, and finally, the constant flow rate Q, the compressibility c, the pore pressure P0 and a pressure P(Rneedle,t) from any particular time t are evaluated in the derived "intermediate time" formula $\varphi = \{16\pi^3 k_{eff}{}^3 t/(Q^2\mu^3 c)\}\{P(R_{needle},t) - P_0 + (Q\mu)/(4\pi R_{needle} k_{eff})\}^2$. From our experience, the results are often unreliable,

since extrapolated keff and P_0 values are also subject to error. Similar problems arise in petroleum analysis, so in practice, rock porosities are obtained from separate nuclear measurements.

Fortunately, anisotropy characterization is more optimistic. Just as directional sound properties in a symphony hall require "two ears," anisotropy tissue estimates depend on tissue data from pressure sensors at two locations. This requires nontrivial hardware modifications. A second micro-transducer must be installed at the needle exterior about 1-2 cm from the needle entry point, so that dual steady-state pressure readings can be obtained for use in derived kh-kv formulas documented in the prior references. Precise flat-mounting is required so that needle penetration does not inflict additional discomfort. This modification requires developmental work now in progress.

Conclusions and Closing Remarks

While we have developed concept and porous media math interpretation models in prior work, the main contributions in the present exploratory study are hardware and software prototyping, and the wealth of experimental data collected in Figures 14-A,B,C,D. The raw, unprocessed pressure curves all show waveforms consistent with theoretical results in Figure 5, additionally emphasizing the generally low permeability nature we anticipated at the outset. Our collection of data, importantly, showed the same consistency throughout all data sets, including those not published here, and it was not necessary to eliminate visually apparent outliers from analysis. Samples tested, of course, were not ideal and uniform – in fact, they were heterogeneous, streaky, grainy and often anisotropic. This motivates the need for multi-needle syringes, for example as shown in Figure 16, that collect suites of location data from broader target zones in single passes. This contributes to a fuller characterization of the sample medium. No effort was made to study any particular sample in detail in this exploratory work.

Our research also suggests the following future areas for study, which include, but are not limited to (1) calibration methods for needles have different radii, blunted or beveled tips, and entry angle so that data falls within the realm interpretable by spherical flow analysis, and identification of off-the-shelf manufactured samples useful for calibration; (2) micro-transducer pressure sensors for external needle placement that facilitate kh and kv individual measurements; (3) improved approaches to measuring porosity, requiring further theoretical development; (4) reduced flow rate methods to minimize patient pain and which preserve tissue integrity in animal and human testing; (5) extended hardware prototyping to handle saline (as opposed to gas) injections; and (6) low cost syringe pump designs, together with wireless data acquisition and iPhone, Android or HuaweiOS based phones to enhance portability. Fulfillment of these objectives would provide an imaging tool useful in characterizing local anomalies quantitatively, rapidly, conveniently and inexpensively, providing an almost fully non-invasive means suitable for routine monitoring, and hence a product that is easily manufactured and deliverable to all worldwide populations developed and under-developed.

Acknowledgements

Guidance and marketing advice from Dr. Nicholas Chen, Double Medical Company, Xiamen, China, and from Mr. Tim Cheung, Techno-Entrepreneurship Core, The University of Hong Kong (HKU), Hong Kong Science and Technology Park (HKSTP) SEED Innovation Program are gratefully acknowledged.

Author Information, Funding Details and Conflicts of Interest

The author is affiliated with the Faculty of Science with Hong Kong University. Original R&D activities, to include idea initiation, algorithm design, book publication and patent applications, were supported by iSyringe Imaging Technologies Limited, Hong Kong, while prototyping and sample testing were partially supported by HKU and HKSTP through their SEED Initiatives. No other conflicts of interest are noted.

References

1. Carreau A, Hafny-Rahbi BE, Matejuk A, Grillon C, Kieda C. Why is the partial oxygen pressure of human tissues a crucial parameter?" Journal of Cellula and Molecular Medicine 15 (2011): 1239-1253.
2. Chanda A, Callaway C. Tissue Anisotropy Modeling Using Soft Composite Materials. Applied Bionics and Biomechanics 2018.
3. Chin WC, Chin JA. Biofluids Modeling – Methods, Perspectives and Solutions, John Wiley and Sons, New York, 2023.
4. Chin WC, Chin JA, Zhuang X. Intelligent Syringe for Porous Tissue Characterization Using Advanced Darcy Flow Pressure Transient Analysis. International Journal of Applied Biology and Pharmaceutical Technology 2024.
5. Chin WC, Zhou Y, Feng Y, Yu Q, Zhao L. Formation Testing – Pressure Transient and Contamination Analysis, John Wiley & Sons, New York, 2014.
6. Doughty DV, Clawson CZ, Lambert W, Anand Subramony J. Understanding Subcutaneous Tissue Pressure for Engineering Injection Devices for Large-Volume Protein Delivery. Journal of Pharmaceutical Sciences 105 (2016): 2105-2113.
7. Duran-Reynals F. Tissue Permeability and the Spreading Factors in Infection. Bacteriol Rev 6 (1942): 197-252.

8. Franke RP, Fuhrmann R, Hiebl B, Mrowietz C, Jung F. Permeability of technical and biological tissues. Clin Hemorheol Microcirc 43 (2009): 149-155

9. Loh QL, Choong C. Three-Dimensional Scaffolds for Tissue Engineering Applications: Role of Porosity and Pore Size. Tissue Eng Part B Rev 19 (2013): 485-502.

10. Mitchell GR, Tojeira A. Role of Anisotropy in Tissue Engineering," Procedia Engineering, Elsevier (59) 2013: 117-125.

11. Nolan DR, Mcgarry JP. On the Compressibility of Arterial Tissue. Annals of Biomedical Engineering 44 (2015).

12. Woodley WD, Morel DR, Sutter DE, Pettis RJ, Bolick NG. Clinical evaluation of large volume subcutaneous injection tissue effects, pain, and acceptability in healthy adults. Clinical and Translational Science 15 (2022).

13. Yuan SY, Rigor RR. Regulation of Endothelial Barrier Function, Chapter 3 – Methods for Measuring Permeability, Morgan & Claypool Life Sciences, San Rafael (CA) 2010.

Citation: Jamie A. Chin. Real-time Tissue Properties from "Intelligent iSyringe" Pressure Transient Analysis. Journal of Radiology and Clinical Imaging 8 (2025): 72-87.